

Complicated nature of the gap in MgB₂: magnetic field-dependent optical studies

H. J. Lee,¹ J. H. Jung,¹ K. W. Kim,¹ M. W. Kim,¹ T. W. Noh,¹ Y. J. Wang,² W. N. Kang,³ Eun-Mi Choi,³ Hyeong-Jin Kim,³ and Sung-Ik Lee³

¹*School of Physics and Research Center for Oxide Electronics, Seoul National University, Seoul 151-747, Korea*

²*National High Magnetic Field Laboratory at Florida State University, FL 32310, USA*

³*National Creative Research Initiative Center for Superconductivity, Department of Physics, Pohang University of Science and Technology, Pohang 790-784, Korea*

(January 30, 2020)

We investigated the magnetic field (H)-dependent optical conductivity spectra of MgB₂ thin film in the far-infrared region. The H -dependences can be explained by the increase of normal metallic regions embedded in the superconducting background. The area fraction of the normal metallic region increases rather quickly at low field, but slowly at high field. It follows neither H - nor $H^{1/2}$ -dependences. The results suggest the complicated nature of the superconducting gap in MgB₂.

PACS number: 74.25Gz, 74.76.Db

The recent discovery of superconductivity in MgB₂ with $T_C = 39$ K¹ has generated a tremendous amount of attention among condensed matter researchers. Many theoretical and experimental efforts have been conducted to understand its superconductivity and the phonon-mediated BCS mechanism² was suggested as being responsible. However, there have been reports of distinctly different values of the superconducting gap 2Δ , i.e., from 3 to 16 meV, which makes understanding its physical properties rather problematic. Also, the experimental evidences for the deviation from an isotropic s-wave gap symmetry have been accumulating and an anisotropic s-wave gap symmetry³ or a multiple gap⁴ have been suggested.

Optical measurements are known to be a powerful tool for investigating important physical quantities, such as 2Δ , the scattering rate $1/\tau$, penetration depth λ , and plasma frequency⁵. Since the skin depth of light is about 1000 Å in the far-infrared region, optical measurements have an important advantage for obtaining bulk properties compared to other surface sensitive techniques, such as tunneling measurements. Also, optical measurements at high magnetic field (H) can provide fruitful information, such as vortex dynamics, quasi-particle excitation, and gap symmetry^{6,7}. There have been only a few reports on the temperature-dependent optical properties of MgB₂^{8–10}. Earlier, we reported the value of $2\Delta(0) \approx 5.2$ meV and $2\Delta(0)/k_B T_C \approx 1.8$ for a *c*-axis oriented MgB₂ thin film⁹. Although our value of $2\Delta(0)/k_B T_C$ was half that of the BCS prediction, we found that 2Δ seemed to follow the temperature dependences of the BCS formula. To obtain further information on the gap nature of MgB₂, we have performed H -dependent optical studies. [As far as we know, this is the first investigation on the optical properties of MgB₂ under high H .]

In this paper, we report H -dependent complex optical conductivity spectra $\tilde{\sigma}(\omega)$ of MgB₂ thin film. In the su-

perconducting state, the superconductivity became suppressed under the external H . The $\tilde{\sigma}(\omega)$ of this mixed state can be modeled with the Maxwell-Garnett theory, which assumes that the normal metallic regions are embedded in a superconducting background. Using the composite medium theory, the H -dependent $\tilde{\sigma}(\omega)$ could be explained quite well. Interestingly, the area fraction of the normal metallic region showed neither an H dependent characteristic of an *s*-wave superconductor (i.e., a linear dependence) nor that of a *d*-wave superconductor (i.e., $H^{1/2}$ dependence). It increased rapidly at low field, but rather slowly at high field. This intriguing result suggests the existence of a complicated gap nature for MgB₂.

We measured far-infrared transmission $T(\omega)$ and reflectivity $R(\omega)$ spectra of a MgB₂ thin film (thickness ~ 200 Å) at various H from 0 to 17 T. A high quality *c*-axis oriented MgB₂ film was grown on an Al₂O₃ substrate by the pulsed laser deposition technique¹¹. The *dc* resistivity measurement showed a sharp T_C near 33 K. For optical measurements, the sample was cooled down to 4.2 K at zero field and then H was applied along the *c*-axis. Using the Bruker spectrophotometer, $T(\omega)$ and $R(\omega)$ were carefully measured over the range $30 \sim 200$ cm⁻¹. For $T(\omega)$ mode, we measured center area and for $R(\omega)$, whole area of the film.

Figure 1(a) shows the H -dependent $T(\omega)$ at 4.2 K. At 0 T, $T(\omega)$ show a peak structure near 50 cm⁻¹, which is closely related to 2Δ ⁹. With increasing H , the peak structure becomes suppressed and the peak position moves to higher frequencies¹². At 17 T, the peak disappears and $T(\omega)$ show a flat response, i.e., normal metallic behavior. The corresponding H -dependent $R(\omega)$ are shown in Fig. 1(b). At 0 T, $R(\omega)$ show a deep structure near 60 cm⁻¹. With increasing H , the deep structure in $R(\omega)$ becomes broader and finally flattens at 17 T. It is interesting to note that significant changes in $T(\omega)$ and

$R(\omega)$ occur below 2 T¹³.

We obtained $\tilde{\sigma}(\omega)$ ($= \sigma_1(\omega) + i\sigma_2(\omega)$) from $T(\omega)$ and $R(\omega)$ in Fig. 1 by solving the appropriate Fresnel equations for a film geometry¹⁴. The light reflects multiply both inside the film and the substrate. The multiple reflections inside the film should be added coherently. However, because the thickness of the substrate was much larger than the wavelength of the incident light, the phase coherence can easily be lost due to surface imperfections such as roughness, which will lead to the decrease of the Fabry-Pérot fringes. To avoid such a problem, the optical measurements were conducted with a low resolution (i.e., 4.0 cm⁻¹) and the multiple reflections inside the substrate were added incoherently in the calculation.

Figure 2(a) shows the H -dependent $\sigma_1(\omega)$. At 0 T, $\sigma_1(\omega)$ show a deep structure around 44 cm⁻¹ related with 2Δ and a sharply increasing behavior above 2Δ . With increasing H , the deep structure becomes smooth and $\sigma_1(\omega)$ at 17 T slowly decrease with increasing frequency. It should be noted that the position of the deep structure increases as H increases, which is opposite to the temperature dependence of 2Δ ⁹. Figure 2(b) shows the H -dependent $\sigma_2(\omega)$. At 0 T, $\sigma_2(\omega)$ show a $1/\omega$ -dependence due to the delta-function of $\sigma_1(0)$. $\sigma_2(\omega)$ at 4 T show a peak-like feature around 50 cm⁻¹ and $\sigma_2(\omega)$ at 17 T slowly increase with increasing frequency. Note that the $\tilde{\sigma}(\omega)$ at 0 T and 17 T are similar to the reported behavior of the superconducting (i.e., 5 K) and the normal metallic (i.e., 40 K) states, respectively¹⁰. From Fig. 2, we obtained $\sigma_1(0) \sim 20000 \Omega^{-1}\text{cm}^{-1}$ and $1/\tau \sim 800 \text{ cm}^{-1}$ in the normal state, and $2\Delta \sim 44 \text{ cm}^{-1}$ and $\lambda \sim 2000 \text{ \AA}^{15}$ in the superconducting state.

Such strong H -dependent $\sigma_1(\omega)$ and $\sigma_2(\omega)$ should be related to the evolution of a vortex in a type-II superconductor. Below H_{c1} , the magnetic flux cannot penetrate into the superconductor, which is the Meissner effect. Above H_{c1} , the magnetic flux starts to penetrate into the superconductor, forming a vortex. Inside the vortex, the superconducting regions become suppressed and turn into normal metallic regions. With increasing H , the number of vortexes increases. Above H_{c2} , the superconducting properties are totally destroyed¹⁶. The values of H_{c1} and H_{c2} for MgB₂ were reported to be around 450 Oe¹⁷ and 20 T¹⁸, respectively.

Optical responses of a type-II superconductor under high H have been rarely investigated and there has not been much systematic analysis⁷. To explain the optical responses shown in Figs. 2(a) and 2(b), we used the composite medium theory, called the Maxwell Garnett theory (MGT). In the long wavelength limit, the physical properties of the composite can be described in terms of an effective dielectric constant, $\tilde{\epsilon}^{eff}$. Since the vortexes are well isolated from each other due to the inter-vortex Coulomb repulsion, as an approximation, we can consider our film as a composite system composed of normal metal disks embedded in a superconductor. Then, such a geometry can be approximated quite well by the two-dimensional MGT¹⁹: $\tilde{\epsilon}^{eff}$ ($= 4\pi i\tilde{\sigma}^{eff}/\omega$) can be written

as,

$$\tilde{\epsilon}^{eff} = \tilde{\epsilon}^s \frac{(1 - f_n)\tilde{\epsilon}^s + (1 + f_n)\tilde{\epsilon}^n}{(1 + f_n)\tilde{\epsilon}^s + (1 - f_n)\tilde{\epsilon}^n}, \quad (1)$$

where $\tilde{\epsilon}^s$ and $\tilde{\epsilon}^n$ represent the complex dielectric constants of the superconducting and normal metallic regions, respectively, and f_n represents the area fraction of the metallic regions. For $\tilde{\epsilon}^s$, we used the Zimmerman formula²⁰, i.e., the optical response of the BCS superconductor, with $2\Delta = 44 \text{ cm}^{-1}$ and $1/\tau = 800 \text{ cm}^{-1}$. For $\tilde{\epsilon}^n$, we used the simple Drude model with $\sigma_1(0) = 20000 \Omega^{-1}\text{cm}^{-1}$ and $1/\tau = 800 \text{ cm}^{-1}$.

In Figs. 2(c) and 2(d), we show the calculated $\sigma_1^{eff}(\omega)$ and $\sigma_2^{eff}(\omega)$, respectively. It is clear that the calculated $\sigma_1^{eff}(\omega)$ and $\sigma_2^{eff}(\omega)$ are quite similar to the measured spectra. As shown in Figs. 1(a) and 1(b), the calculated $T^{eff}(\omega)$ and $R^{eff}(\omega)$ from $\tilde{\sigma}^{eff}(\omega)$ can also fit the experimental data quite well. These results show that the MGT can describe the electrodynamic responses of a type-II superconductor under high H quite well.

The area fraction of the normal metallic regions for the MgB₂ film shows quite an unusual H -dependent behavior. In Fig. 3(a), we plotted the H -dependent f_n , estimated by comparing the experimental data with the calculated values, with error bars. f_n increases sharply at low field and slowly at high field; for example, more than half of the film becomes metallic below $\sim 2 \text{ T} \ll H_{c2}$. It is known that the values of f_n can be obtained from a heat capacity study by measuring the coefficient γ . For an *s*-wave superconductor, γ is known to be proportional to H^{21} . On the other hand, for a superconductor with a node on the gap, for example, a *d*-wave symmetry, γ should be proportional to $H^{1/222}$. The dashed and solid lines in Fig. 3 (a) show the H -dependent f_n for *s*- and *d*-waves, respectively. Neither of these H -dependencies can explain our experimental data. Fig. 3(b) shows the plot of $\log(f_n)$ vs. $\log(H)$. [The error bars are smaller than the size of the symbols.] The two H regions with different slopes are clearly seen. Interestingly, f_n below and above 2 T seems to follow the power law dependences of $H^{0.75}$ and $H^{0.33}$, respectively.

Recently, Bouquet *et al.*²³ observed a rapid increase of γ at low H and a saturation behavior at high H , which are in qualitative agreement with our observed behavior of f_n . To explain this behavior, they suggested the existence of two gaps. Szabo *et al.*⁴ also reported the existence of two superconducting energy gaps using point-contact spectroscopy measurements. Values of the small gap $2\Delta_S$ and large gap $2\Delta_L$ were reported to be 5.6 meV and 14 meV, respectively. Both superconducting gaps were shown to follow the temperature dependence of the BCS formula. However, $2\Delta_S$ becomes strongly suppressed with H below 1.0 T.

There is some consistency between our observations and earlier works proposing the two gap scenario²⁴. Our observed value of $2\Delta \approx 5.4 \text{ meV}$ ($2\Delta/k_B T_C \approx 1.9$) in the *ab*-plane and its BCS temperature dependence seem to be

consistent with the characteristics of the small gap in the two gap scenario. Moreover, its strong H -dependence at low field seems to agree with the results of Szabo *et al.* As shown in Fig. 3(b), the H -dependence of f_n seems to have a crossover near 2 T. To explain this behavior in the two gap scenario, we assumed that the reported value of H_{c2} , i.e., about 20 T, corresponds to the large superconducting gap. With a crude approximation of $H_{c2} \sim 1/\xi^2 \sim \Delta^2$, the corresponding H_{c2} value for the small superconducting gap, if it exists, will be around 2 T since $2\Delta_S \sim 5.4$ meV. Then, the crossover behavior in Fig. 3(b) could be explained in terms of a more rapid suppression of $2\Delta_S$ under H in the two gap scenario²⁵.

However, a simple two gap scenario based on two independent BCS-like carriers with different gap values cannot explain our optical data. To clarify this statement, we simulated $T(\omega)$ and $R(\omega)$ using the two-fluid model, where the total optical conductivity spectra $\tilde{\sigma}_t(\omega)$ can be written as

$$\tilde{\sigma}_t(\omega) = f_S \tilde{\sigma}_S(2\Delta_S, \omega) + (1 - f_S) \tilde{\sigma}_L(2\Delta_L, \omega), \quad (2)$$

where $\tilde{\sigma}_S(2\Delta_S, \omega)$ and $\tilde{\sigma}_L(2\Delta_L, \omega)$ represent the optical conductivity spectra with the small and large gaps, respectively, and f_S represents the fraction of the superconducting carriers with Δ_S . As shown in Figs. 4(a) and 4(b), the experimental $T(\omega)$ and $R(\omega)$ at $H = 0$ T can be explained rather well only with $f_S \approx 1.0$. Note that all of the earlier optical works on MgB₂ reports a small size gap only⁸⁻¹⁰.

The apparent emergence of only the small gap feature in the optical spectra as well as the unusual H -dependence of f_n put new constraints on understanding the MgB₂ superconducting gap in the two gap scenario²⁵. Although the H -dependence of f_n seems to be consistent with the two gap picture, any two gap model does not explain why only the small gap can be observed in the optical spectra of the *ab*-plane at $H = 0$ T yet. The seemingly contradictory experimental facts suggest that the nature of the superconducting gaps in MgB₂ should be related, which will provide a complicated nature of the gap in the MgB₂. To clarify the complicated gap nature of MgB₂, further studies are needed.

In summary, we have investigated the magnetic field-dependent optical conductivity spectra of the MgB₂ thin film. The magnetic field-dependent optical conductivity spectra could be explained by the Maxwell Garnett theory, which assumes an increase of normal metallic regions embedded in a superconducting background. The area fraction of the normal metallic state was estimated and found to increase rather rapidly at low field but slowly at high field. This magnetic field dependence provides a new constraint to understand the multigap behavior of MgB₂.

We thank H. K. Lee, Prof. J. Yu, and Y.-W. Son for useful discussions and help in performing the experiments. This work at SNU and POSTECH was supported by the Ministry of Science and Technology of Korea through the Creative Research Initiative Program.

This research was conducted at the National High Magnetic Field Laboratory, which is supported by NSF Cooperative Agreement No. DMR-0084173 and by the State of Florida.

¹ J. Nagamatsu, N. Nakagawa, T. Muranaka, Y. Zenitani, and J. Akimitsu, *Nature (London)* **410**, 63 (2001).

² S. L. Bud'ko, G. Lapertot, C. Petrovic, C. E. Cunningham, N. Anderson, and P. C. Canfield, *Phys. Rev. Lett.* **86**, 1877 (2001); J. Kortus, I. I. Mazin, K. D. Belashchenko, V. P. Antropov, and L. L. Boyer, *Phys. Rev. Lett.* **86**, 4656 (2001); J. M. An and W. E. Pickett, *Phys. Rev. Lett.* **86**, 4366 (2001).

³ P. Seneor, C.-T. Chen, N.-C. Yeh, R. P. Vasquez, L. D. Bell, C. U. Jung, M.-S. Park, H.-J. Kim, W. N. Kang, and S.-I. Lee, *Phys. Rev. B* **65**, 012505 (2002); S. Haas and K. Maki, *Phys. Rev. B* **65**, 020502 (2002).

⁴ P. Szabo, P. Samuely, J. Kacmarik, T. Klein, J. Marcus, D. Fruchart, S. Miraglia, C. Marcenat, and A. G. M. Jansen, *Phys. Rev. Lett.* **87**, 137005 (2001); F. Giubileo, D. Roditchev, W. Sacks, R. Lamy, D. X. Thanh, J. Klein, S. Miraglia, D. Fruchart, and J. Marcus, *Phys. Rev. Lett.* **87**, 177008 (2001).

⁵ K. Kamarás, S. L. Herr, C. D. Porter, N. Tache, D. B. Tanner, S. Etemad, T. Venkatesan, E. Chase, A. Inam, X. D. Wu, M. S. Hegde, and B. Dutta, *Phys. Rev. Lett.* **64**, 84 (1990); P. F. Henning, C. C. Homes, S. Maslov, G. L. Carr, D. N. Basov, B. Nikolić, and M. Strongin, *Phys. Rev. Lett.* **83**, 4880 (1999); D. Dulić, A. Pimenov, D. van der Marel, D. M. Broun, S. Kamal, W. N. Hardy, A. A. Tsvetkov, I. M. Sutjaha, R. Liang, A. A. Menovsky, A. Loidl, and S. S. Saxena, *Phys. Rev. Lett.* **86**, 4144 (2001).

⁶ K. Karräi, E. J. Choi, F. Dunmore, S. Liu, H. D. Drew, Q. Li, D. B. Tanner, Y. D. Zhu, and F. C. Zhang, *Phys. Rev. Lett.* **69**, 152 (1992).

⁷ E.-J. Choi, K. P. Stewart, S. K. Kaplan, H. D. Drew, S. N. Mao, and T. Venkatesan, *Phys. Rev. B* **53**, R8859 (1996); A. Zibold, H. L. Liu, D. B. Tanner, J. Y. Wang, M. Gruninger, H. P. Geserich, T. Kopp, Th. Wolf, W. Widder, and H. F. Braun, *Phys. Rev. B* **55**, 11 096 (1997).

⁸ B. Gorshunov *et al.*, *European J. Phys. B* **21**, 159 (2001); A. V. Pronin, A. Pimenov, A. Loidl, and S. I. Krasnosvobodtsev, *Phys. Rev. Lett.* **87**, 097003 (2001); J. J. Tu, G. L. Carr, V. Perebeinos, C. C. Homes, M. Strongin, P. B. Allen, W. N. Kang, E.-M. Choi, H.-J. Kim, and S.-I. Lee, *Phys. Rev. Lett.* **87**, 277001 (2001).

⁹ J. H. Jung, K. W. Kim, H. J. Lee, M. W. Kim, T. W. Noh, W. N. Kang, H.-J. Kim, E.-M. Choi, C. U. Jung, and S.-I. Lee, *Phys. Rev. B* **65**, 052413 (2002).

¹⁰ R. A. Kaindl, M. A. Carnahan, J. Orenstein, D. S. Chemla, H. M. Christen, H.-Y. Zhai, M. Paranthaman, and D. H. Lowndes, *Phys. Rev. Lett.* **88**, 027003 (2002).

¹¹ W. N. Kang, H.-J. Kim, E.-M. Choi, C. U. Jung, and S.-I. Lee, *Science* **292**, 1521 (2001).

¹² At $H = 0$ T, the peak position of $T(\omega)$ [ref. 9] gradually

shifts towards the lower frequency as the temperature increases.

¹³ The optical constants of Al_2O_3 substrate are nearly H -independent in the far-infrared region.

¹⁴ J. S. Ahn, J. Bak, H. S. Choi, T. W. Noh, J. E. Han, Y. Bang, J. H. Cho, and Q. X. Jia, Phys. Rev. Lett. **82**, 5321 (1999); H. S. Choi, J. S. Ahn, J. H. Jung, T. W. Noh, and D. H. Kim, Phys. Rev. B **54**, 4621 (1996).

¹⁵ To evaluate superconducting penetration depth, we used $\lambda = (\mu_0\omega\sigma_2(\omega, T))^{-1/2}$ with the value of σ_2 at lowest wavenumber. Here μ_0 represents the magnetic susceptibility at vacuum.

¹⁶ M. Tinkham, *Introduction to superconductivity*, (McGraw-Hill, New York, 1996).

¹⁷ A. Sharoni, I. Felner, and O. Millo, Phys. Rev. B **63**, 220508 (2001).

¹⁸ M. H. Jung, M. Jaime, A. H. Lacerda, G. S. Boebinger, W. N. Kang, Hyeong-Jin. Kim, Eun-Mi Choi, and Sung-Ik Lee, Chem. Phys. Lett. **343**, 447 (2001).

¹⁹ J. C. Maxwell-Garnett, Philos. Trans. Roy. Soc. **203**, 307 (1904); T. W. Noh, S. G. Kaplan, and A. J. Sievers, Phys. Rev. B **41**, 307 (1990).

²⁰ W. Zimmermann, E. H. Brandt, M. Bauer, E. Seider, and L. Genzel, Physica C **183**, 99 (1991).

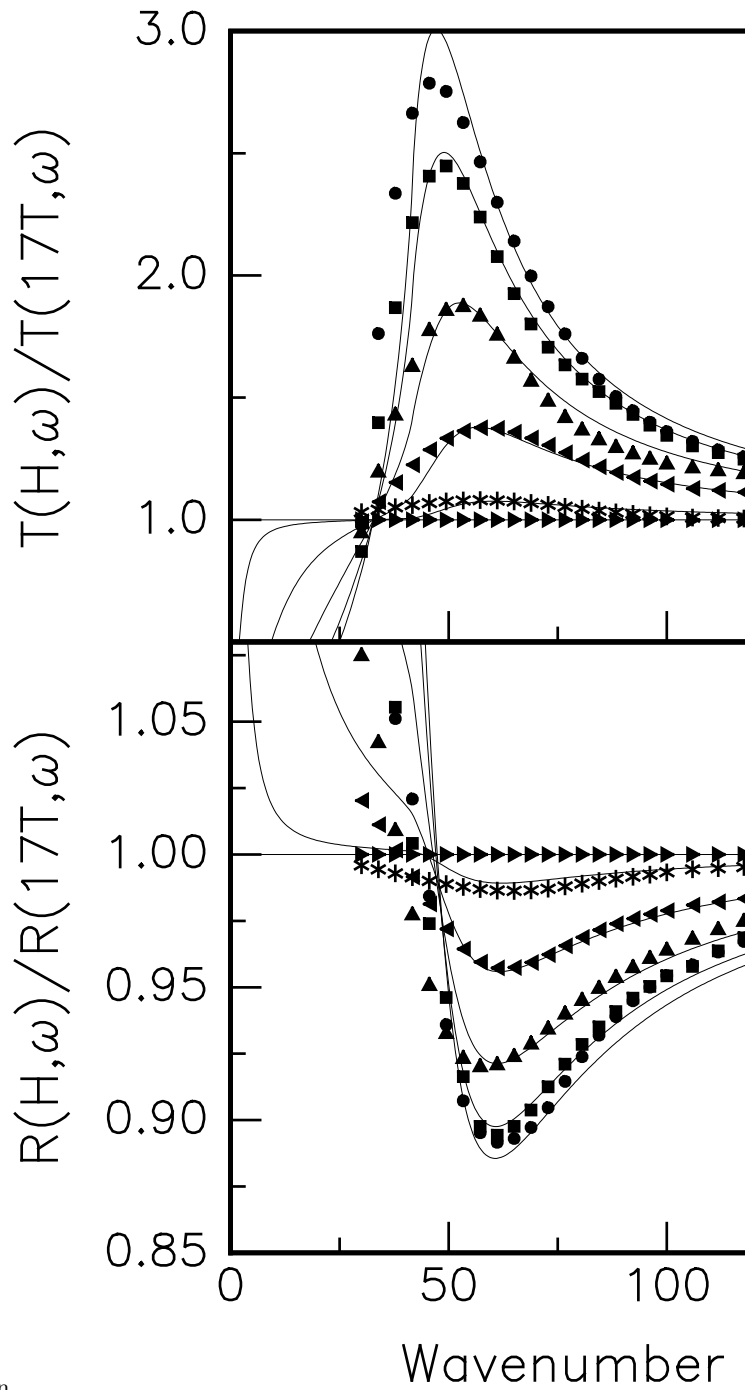
²¹ C. Caoli, P. G. de Gennes, and J. Matricon, Phys. Lett. **9**, 307 (1964).

²² G. E. Volovik, JETP Lett. **58**, 469 (1993).

²³ F. Bouquet, R. A. Fisher, N. E. Phillips, D. G. Hinks, and J. D. Jorgensen, Phys. Rev. Lett. **87**, 047001 (2001).

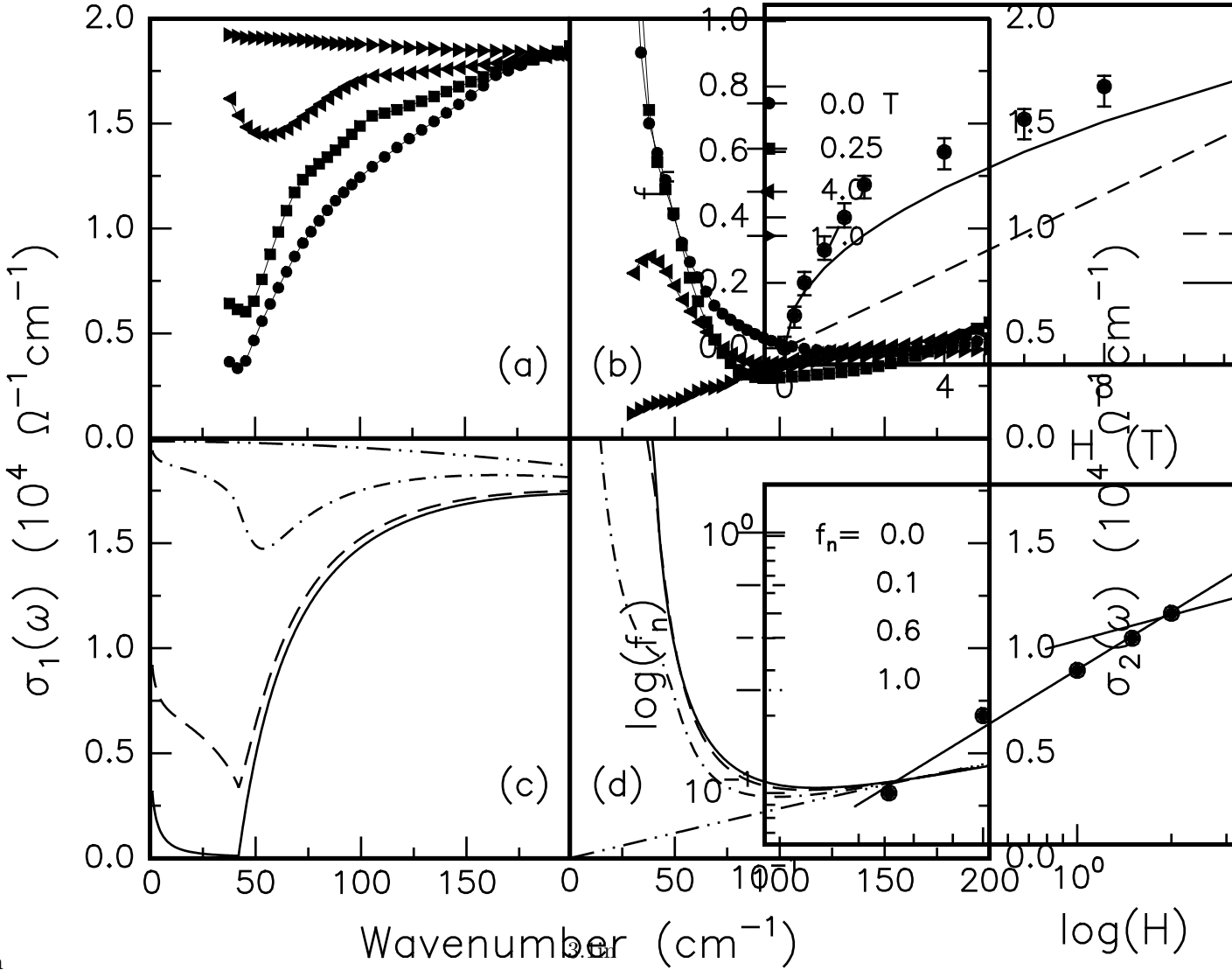
²⁴ A.Y. Liu, I. I. Mazin, and J. Kortus, Phys. Rev. Lett. **87**, 087005 (2001).

²⁵ In the anisotropic s-wave scenario (Ref. 3), where the large gap could be along the c -axis, the strong suppression of f_n under low H cannot be explained.



3.1in

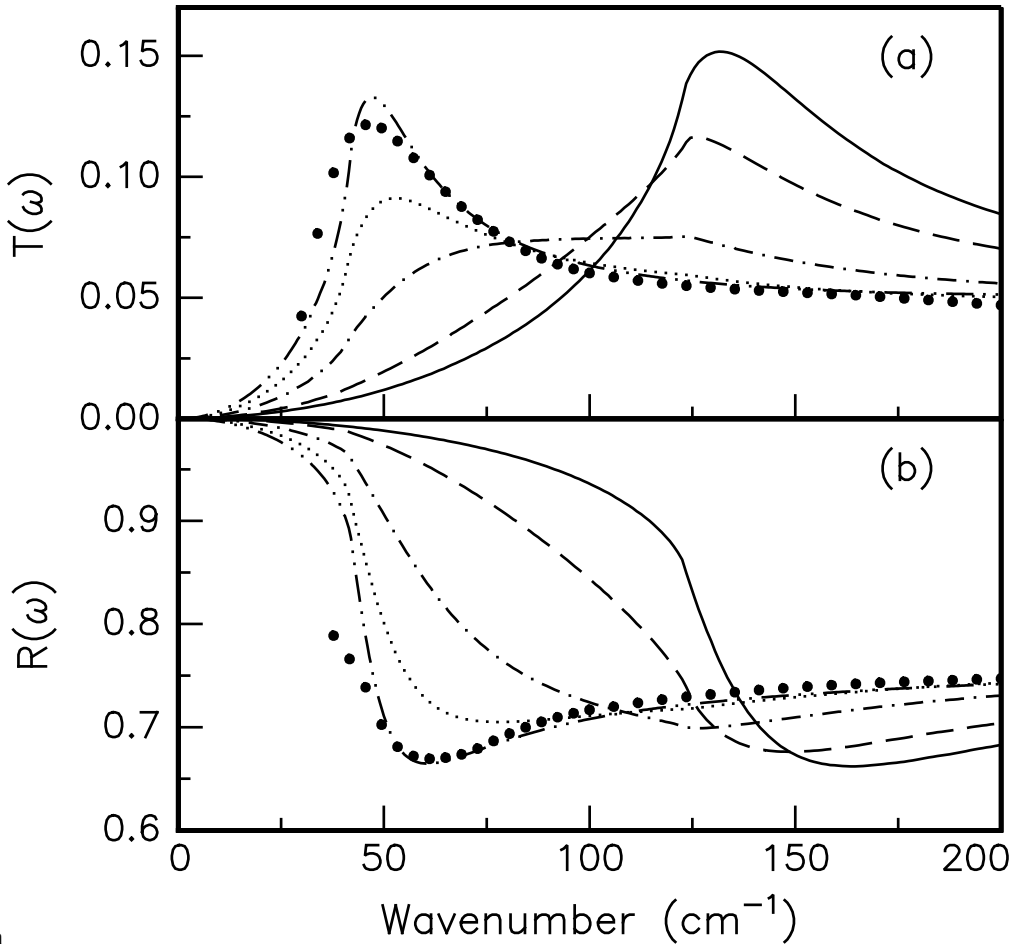
FIG. 1. Experimental (symbols) and theoretical (solid lines) (a) $T(\omega)$ and (b) $R(\omega)$ for MgB_2 thin film at some selected fields.



3.1in

FIG. 2. H -dependent (a) $\sigma_1(\omega)$ and (b) $\sigma_2(\omega)$. In (c) and (d), the calculated $\sigma_1^{\text{eff}}(\omega)$ and $\sigma_2^{\text{eff}}(\omega)$ using Maxwell Garnett Theory are shown, respectively. Here, f_n represents the area fraction of normal metallic region.

FIG. 3. (a) H -dependences of f_n . The dashed and solid lines represent the power law dependences of H and $H^{1/2}$, respectively. In (b), we show the log-log plot of f_n and H . The solid lines represent the least-square fits. The exponents are 0.75 and 0.33 for below and above 2 T, respectively.



3.1in

FIG. 4. (a) $T(\omega)$ and (b) $R(\omega)$ for various fractions (f_S) of the small gap. The solid circles represent the experimental data at 0 T. The solid, dashed, dot-dashed, dotted, and dot-dot-dashed lines represent the corresponding spectra for $f_S = 0.0, 0.3, 0.7, 0.9$, and 1.0 , respectively.